N93-19433

128452

P- 15

Parameter and Configuration Study of the DSS-13 Antenna Drives

W. Gawronski and J. A. Mellstrom
Ground Antennas and Facilities Engineering Section

The effects of different elevation and azimuth drive configurations on DSS-13 antenna performance are presented as well as a study of gearbox stiffness and motor inertia. Small motor inertia and rigid gearboxes would improve the pointing accuracy up to a certain limit. The limit is imposed by critical values of gearbox stiffness and motor inertia introduced in the article. The critical values depend on the lowest structural frequency of the rate-loop model. The tracking performance can be improved by raising gearbox stiffness to the critical stiffness and reducing motor inertia to the critical inertia. An azimuth drive configuration with four driven wheels was also investigated. For the four-wheel drive configuration in azimuth, the cross-coupling effects are reduced and wind disturbance rejection properties improved. Pointing is improved substantially in the cross-elevation but is relatively unaffected in the elevation direction. More significant improvements can be achieved through either structural redesign (stiffening the structure) or new control algorithms or control concepts, which would eliminate the effect of flexible deformations on the antenna pointing accuracy. Although the study is performed for the DSS-13 antenna, the results can be extended for other DSN antennas.

I. Introduction

This article investigates the DSS-13 antenna drives and their effect on antenna pointing accuracy. Each elevation and azimuth drive consists of a pair of motors and gearboxes. The size of a motor and a gearbox is determined from such criteria as static wind loads, which do not directly reflect pointing performance. The purpose of this study was to determine criteria for sizing motors and gearboxes so that the pointing accuracy is accounted for. For control system design purposes, the motor size is given in terms of motor inertia, while the gearbox size is given in terms of gearbox stiffness. Gearbox inertia is neglected since it is less than 10 percent of motor inertia when the

gear ratio is taken into account. Different locations of drives in azimuth and elevation are also investigated. One drive in elevation and two drives in azimuth are compared with two smaller drives in elevation and four smaller drives in azimuth, each at a different location. The effect of this drive configuration on antenna pointing accuracy is investigated.

II. Performance Criteria

Tracking performance and wind disturbance rejection are used to evaluate the pointing performance of motors and gearboxes in the elevation and azimuth drives. The

rate-loop bandwidth is used as a measure of tracking performance and rms pointing error due to wind gusts as a measure of wind disturbance rejection. For the purpose of this article, the rate-loop bandwidth is defined as a frequency range from zero up to the lowest lightly damped mode in the rate-loop transfer function (rate command to rate output). This definition is used for the PI controller design, and the lowest lightly damped mode determines the frequency range of the controller action. A lightly damped mode is detected as a resonant peak in the plot of magnitude of the transfer function (Fig. 1). The wider the open-loop bandwidth is, the better the closed-loop tracking performance is. The wind disturbance rejection properties are evaluated through simulations using the antenna model developed in [1] and the wind model described in [2].

III. Parameter Study

In this section, the effect of motor inertia and gearbox stiffness on antenna performance is investigated. It is obvious that a rigid drive would significantly improve a rigid antenna performance. For a flexible antenna, even a rigid drive cannot prevent its flexible deformations, thus the performance improvement through gearbox stiffening is limited. This is analyzed in detail below.

For the DSS-13 antenna performance evaluation (at a 60-deg elevation position), the model developed in [1] is used. The rate-loop model is shown in Fig. 2, where for clarity only the elevation drive is presented. The model consists of the antenna structure model (21 modes, up to 10 Hz, including two free-rotating modes), gearbox model, motor armature, and amplifiers. The elevation and azimuth drive configuration in the rate-loop model is shown in Fig. 3. The nominal motor inertia is $J_{mn} = 0.14$ N m sec^2, (1.236 lb in sec^2), and the nominal gearbox stiffness is $k_{gn} = 1.65 \times 10^6$ N m/rad (1.5×10^7 lb in./rad).

The effect of the gearbox stiffness on the antenna performance is investigated by observing the change of the imaginary components of the rate loop-poles with respect to gearbox stiffness, see Fig. 4. The imaginary parts of the roots represent the structural natural frequencies. Natural frequencies of the structure and the gearbox are shown in this figure. The lowest structural frequency and the gearbox frequency define the bandwidth as shown in Fig. 4. The bandwidth grows with the gearbox stiffness, up to the critical value $k_{gc} = 1.1 \times 10^6$ N m/rad (10^7 lb in./rad). For

$$k_g > k_{gc} \qquad (1)$$

the tracking performance remains unchanged. Thus, the critical stiffness k_{gc} defines the minimal stiffness of a gearbox, which assures reasonable tracking properties.

The bandwidth and the critical stiffness are also seen in the transfer function plots, Fig. 5. For $k_g < k_{gc}$, the gearbox resonant peak, which is smaller than the critical bandwidth, defines the bandwidth (Fig. 5a). For $k_g > k_{gc}$, the bandwidth changes insignificantly (Fig. 5b), since it is determined by the lowest natural frequency of the structure.

The wind disturbance rejection properties have been simulated for x-direction wind (along the elevation axis), and y-direction wind (horizontal direction orthogonal to the elevation axis). The results are summarized in Tables 1 and 2. The tables show that high gearbox stiffness improves wind rejection properties for y-direction wind, while the x-direction wind pointing remains almost unchanged.

The effect of motor inertia on antenna pointing performance is investigated in a similar fashion. The variations of the rate-loop poles due to motor inertia changes have been evaluated, and their imaginary parts are plotted in Fig. 6. The structural natural frequencies and the gearbox frequency are distinguished in this plot. The lowest natural frequency of the structure and the gearbox frequency determine the bandwidth. For

$$J_m > J_{mc} \qquad (2)$$

the bandwidth is constant, and decreases for $J_m > J_{mc}$, deteriorating the antenna tracking properties. Thus, $J_{mc} = 50$ lb in sec^2 is the critical value of inertia. The phenomenon can be observed in the transfer function plots (elevation rate command to elevation rate), Fig. 7, where for small inertia (small when compared with the critical one) the bandwidth is constant and for large inertia the bandwidth narrows.

Tables 1 and 2 summarize wind disturbance rejection properties. They show that the properties do not improve with motor inertia decrease below the critical value.

IV. Configuration Study

The existing drive configuration of the DSS-13 antenna is shown in Fig. 3. It consists of one elevation and two azimuth drives. A new configuration is compared. The number of drives in this configuration is doubled, and they are mounted at different structural locations. Motors are

sized so that their total power is the same as in the original configuration.

Due to the high stiffness of the bullgear, two elevation drives at different locations of the bullgear have the same effect as two drives at the same location. Therefore, two drives are equivalent to one drive with a properly sized motor (the motor inertia of the two-drive configuration is 38 percent of the motor inertia of the one-drive configuration). Hence the two-elevation drive case reduces to the one-drive parameter study presented previously. The transfer function plots in Fig. 7 compare one- and two-elevation drive cases. They show that the bandwidth in azimuth and elevation remains the same. Thus, no improvement in tracking accuracy is observed. Also, simulations show no improvement in the x-direction wind disturbance rejection and moderate improvement in y-direction wind disturbance rejection (assuming rigid enough gearboxes).

Since the stiffness of the alidade is comparable with the stiffness of gearboxes, the problem of four-azimuth drives cannot be reduced to an equivalent two-drive problem. In the four-azimuth-drive configuration, each drive is mounted on a separate azimuth wheel. The same gearbox stiffness is assumed, and the motor inertia is 2.6 times smaller than the motor inertia of the two-drive case. The tracking performance is evaluated through bandwidth comparison of two- and four-azimuth drives (Fig. 8), and through step response simulations (Fig. 9). In Fig. 8(a) the bandwidth in azimuth is slightly larger, and in elevation it remains the same in the four-drive case, while the cross-transfer function (from elevation to azimuth rate and from azimuth to elevation rate) shows significant change. It is confirmed by the closed-loop unit step responses. The responses to an azimuth step command differ slightly for two- and four-azimuth drives, and the responses to an elevation step command overlap in both cases, while cross-coupling responses show significant differences between the four- and two-drive case.

Wind disturbance rejection for the two- and four-azimuth-drive case is compared in Fig. 10 and Tables 3 and 4. The tables show improvement in x-direction wind rejection properties in the four-drive case, but additional stiffening of drives does not improve the wind disturbance rejection properties.

V. Conclusions

The article has defined criteria for drive comparison purposes and determines conditions imposed on gearbox stiffness and motor inertia so that the tracking errors are minimized and wind disturbance rejection properties are improved. It showed the critical values of gearbox stiffness and motor inertia limit tracking performance improvement. The gearbox stiffness should be larger (but not necessarily much larger) than the critical stiffness, and the motor inertia should be smaller (but not necessarily much smaller) than the critical inertia in order to preserve tracking accuracy. The existing (nominal) parameters of the DSS-13 antenna satisfy these demands. An overdesigned drive is a drive with a gearbox stiffness much larger than the critical one and/or motor inertia much smaller than the critical one. Overdesigned drives do not significantly improve the tracking performance, although an overdesigned gearbox improves wind disturbance rejection. Also, the four-azimuth-drive configuration does not improve the tracking performance (bandwidth remains almost unchanged), but improves the cross-dynamic properties and wind disturbance rejection properties for winds from y-direction.

Improvements due to stiffening gearboxes to downsizing drive motors, and to multiple drives are non-negligible, but not dramatic. Thus, for moderate improvement of performance it is advised to stiffen the gearboxes and use four-azimuth drives. Significant improvement may be achieved only through more innovative approaches, such as antenna structure redesign (more rigid), application of a new control algorithm (with vibration suppression properties), or implementation of either new or additional sensors/actuators (e.g., active truss members for structural vibration damping).

References

[1] W. Gawronski and J. A. Mellstrom, "Modeling and Simulations of the DSS-13 Antenna Control System," *TDA Progress Report 42-106*, vol. April–June 1991, Jet Propulsion Laboratory, Pasadena, California, pp. 205–248, August 15, 1991.

[2] W. Gawronski, B. Bienkiewicz, and R. E. Hill, "Pointing-Error Simulations of the DSS-13 Antenna Due to Wind Disturbances," *TDA Progress Report 42-108*, vol. October–December 1991, Jet Propulsion Laboratory, Pasadena, California, pp. 109–134, February 15, 1992.

Table 1. Pointing errors due to x-direction wind.

Drive parameters	k_{gn}, J_{mn}	$10k_{gn}$, J_{mn}	k_{gn}, $0.5J_{mn}$
Elevation pointing error, mdeg	2.81	2.30	2.89
Cross-elevation pointing error, mdeg	1.64	2.01	1.69
X-band loss, dB	0.03	0.03	0.03
Ka-band loss, dB	0.44	0.39	0.46

Table 2. Pointing errors due to y-direction wind.

Drive parameters	k_{gn}, J_{mn}	$10k_{gn}$, J_{mn}	k_{gn}, $0.5J_{mn}$
Elevation pointing error, mdeg	3.77	2.09	4.10
Cross-elevation pointing error, mdeg	0.55	0.32	0.77
X-band loss, dB	0.04	0.01	0.05
Ka-band loss, dB	0.60	0.19	0.72

Table 3. Pointing errors due to x-direction wind disturbances for two- and four-azimuth drives.

Drive parameters	2AZ, k_{gn}	4AZ, k_{gn}	2AZ, $10k_{gn}$	4AZ, $10k_{gn}$
Elevation pointing error, mdeg	2.81	2.43	2.51	2.40
Cross-elevation pointing error, mdeg	1.64	0.43	2.08	0.36
X-band loss, dB	0.03	0.02	0.03	0.02
Ka-band loss, dB	0.44	0.25	0.44	0.24

Table 4. Pointing errors due to y-direction wind disturbances for two- and four-azimuth drives.

Drive parameters	2AZ, k_{gn}	4AZ, k_{gn}	2AZ, $10k_{gn}$	4AZ, $10k_{gn}$
Elevation pointing error, mdeg	3.77	3.77	3.51	3.92
Cross-elevation pointing error, mdeg	0.55	0.53	0.34	0.50
X-band loss, dB	0.04	0.04	0.04	0.04
Ka-band loss, dB	0.60	0.60	0.52	0.65
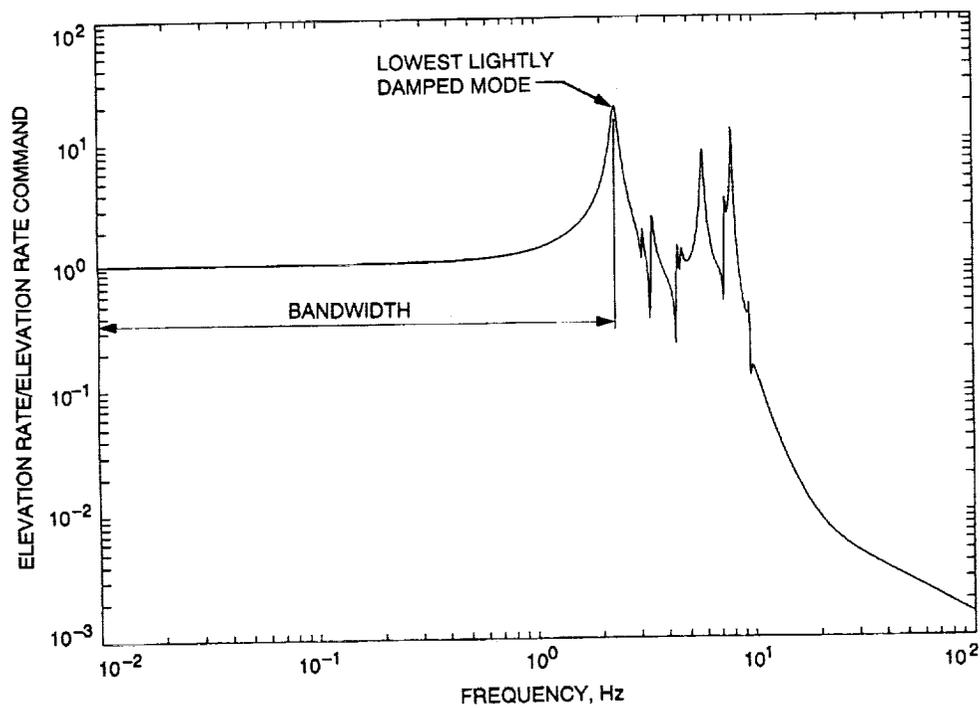
Fig. 1. Bandwidth of the antenna.
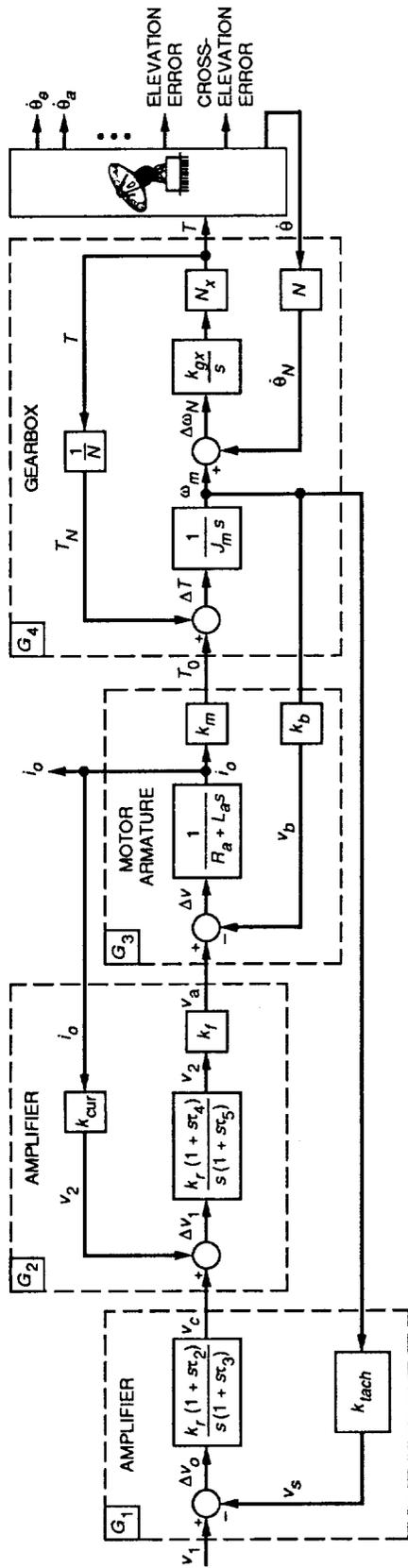
Fig. 2. Rate-loop model of the antenna with the elevation drive.
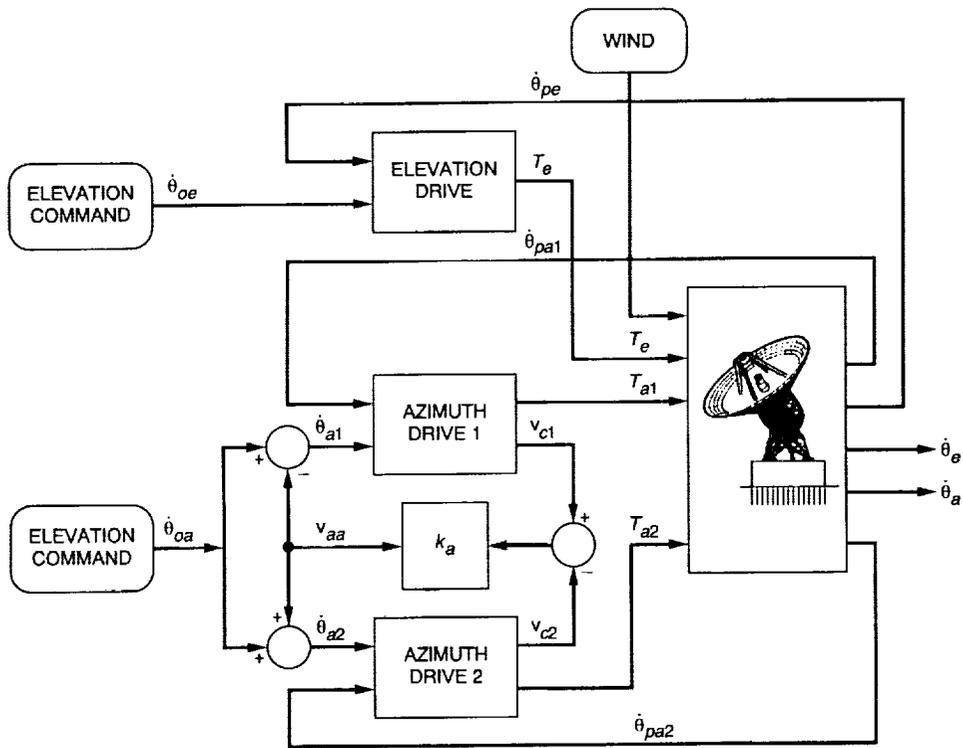
Fig. 3. Rate-loop model of the antenna.
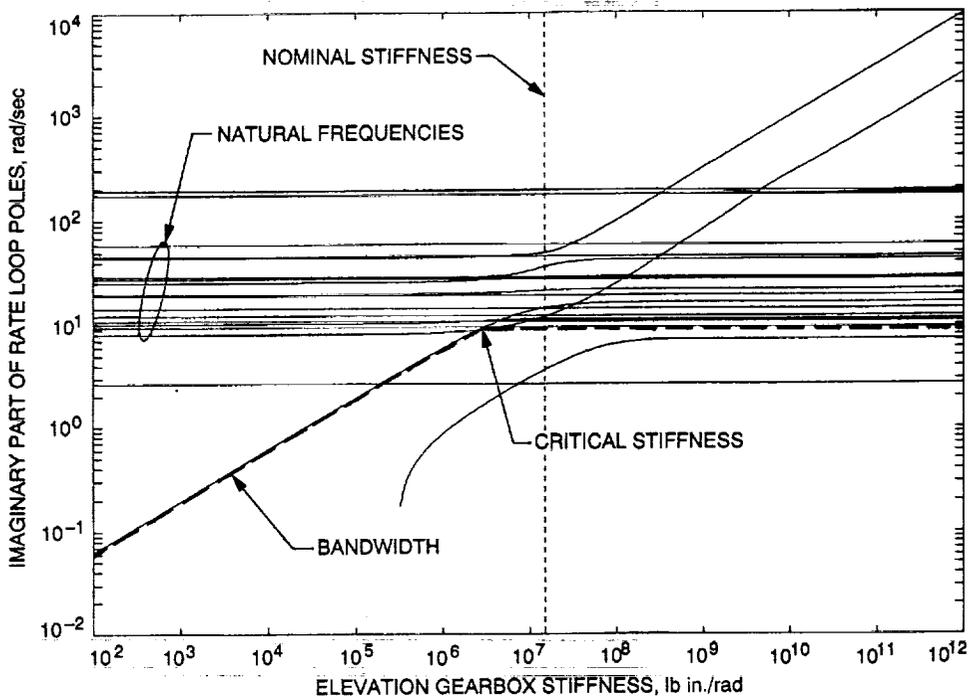
Fig. 4. Imaginary parts of the rate-loop poles versus elevation gearbox stiffness.
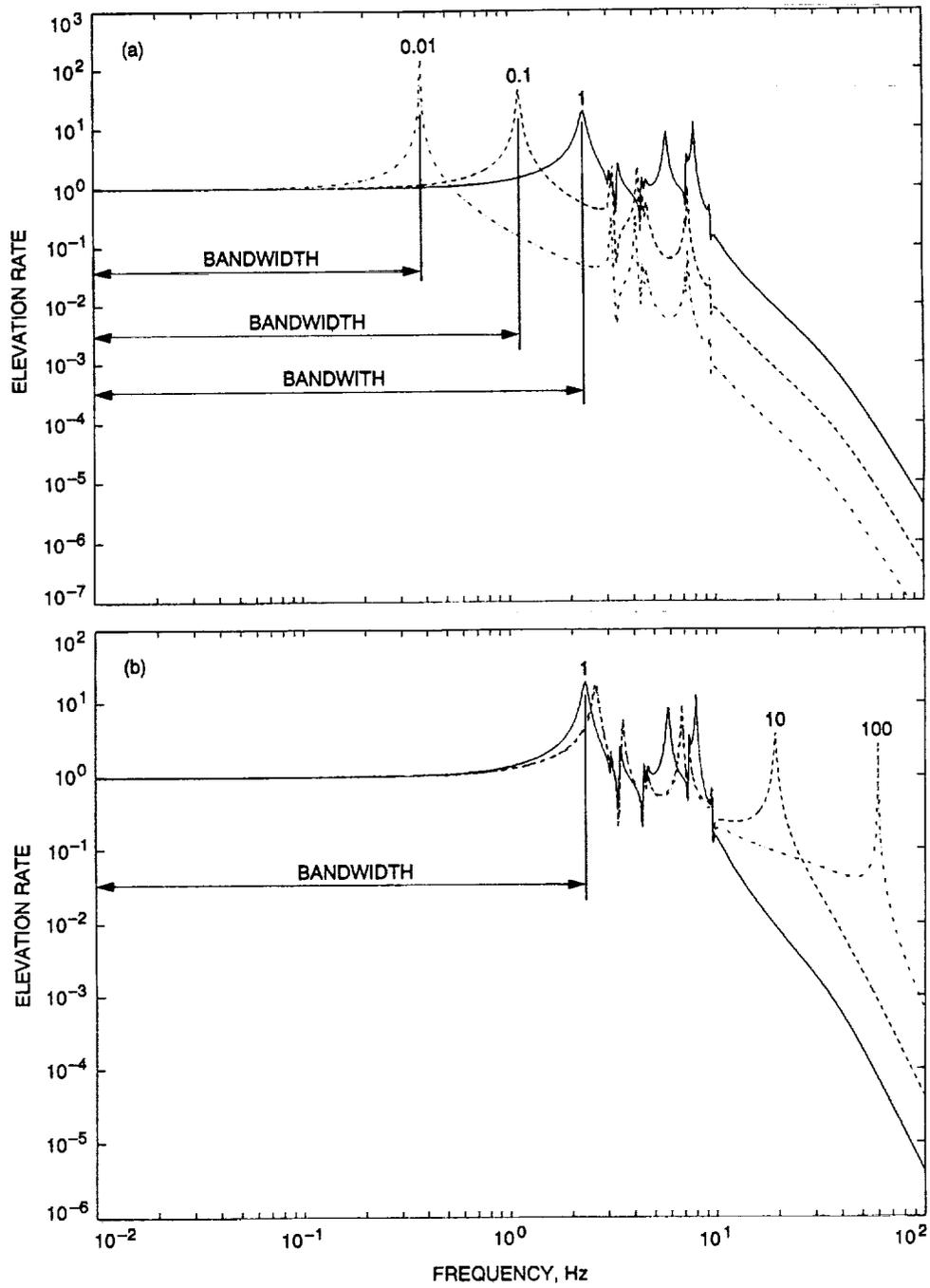
Fig. 5. Transfer functions: elevation rate output to elevation rate command.
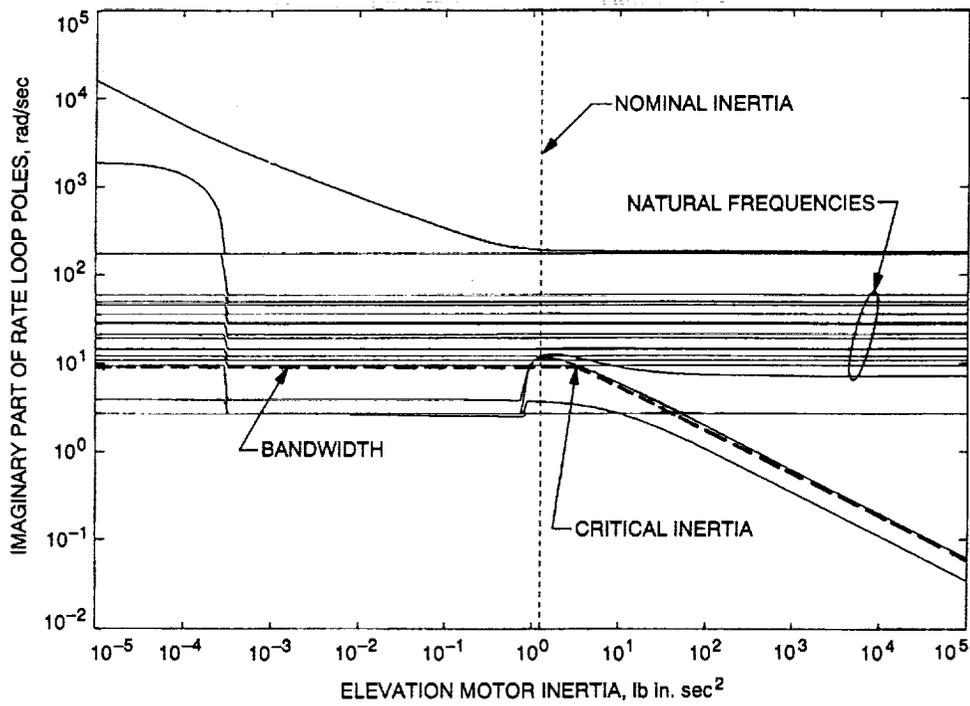
Fig. 6. Imaginary parts of the rate-loop poles versus elevation motor inertia.
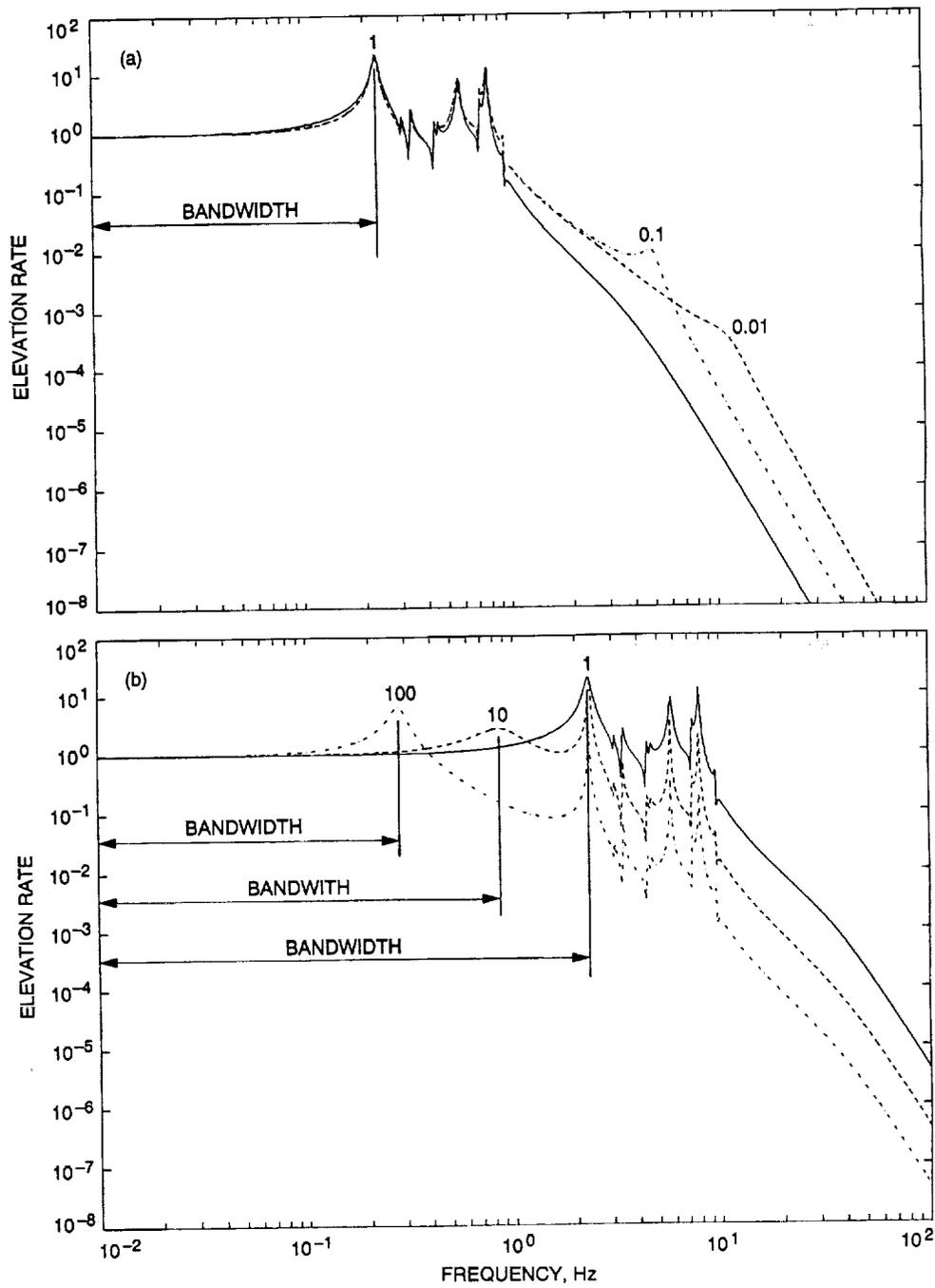
Fig. 7. Transfer functions: elevation rate output to elevation rate command.
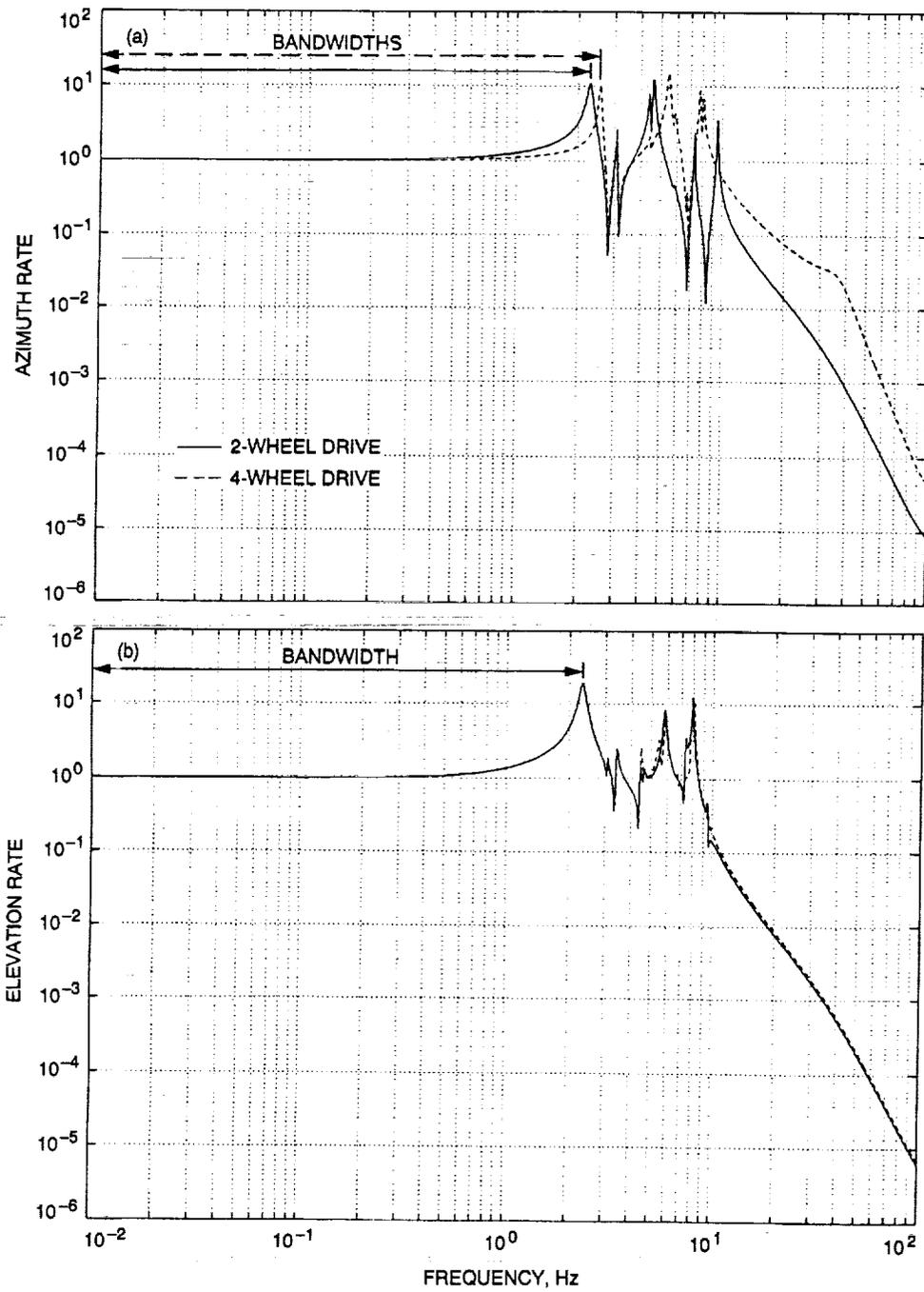
Fig. 8. Bandwidth for two- and four-wheel azimuth drives: (a) azimuth rate to azimuth rate command and (b) elevation rate to elevation rate command.
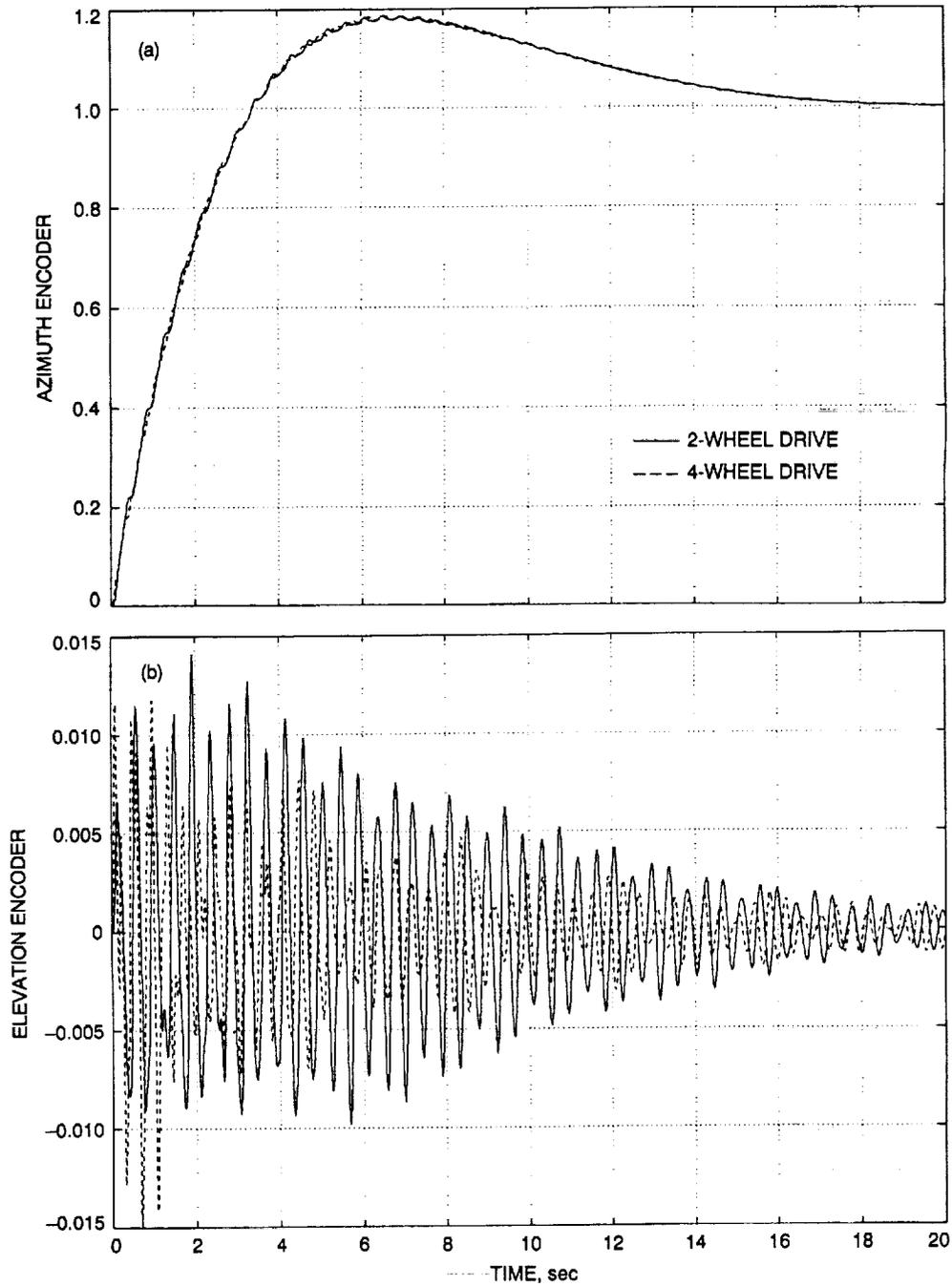
Fig. 9. Step responses for two- and four-wheel azimuth drives: (a) azimuth encoder to azimuth command; (b) elevation encoder to azimuth command; (c) elevation encoder to elevation command; and (d) azimuth encoder to elevation command.
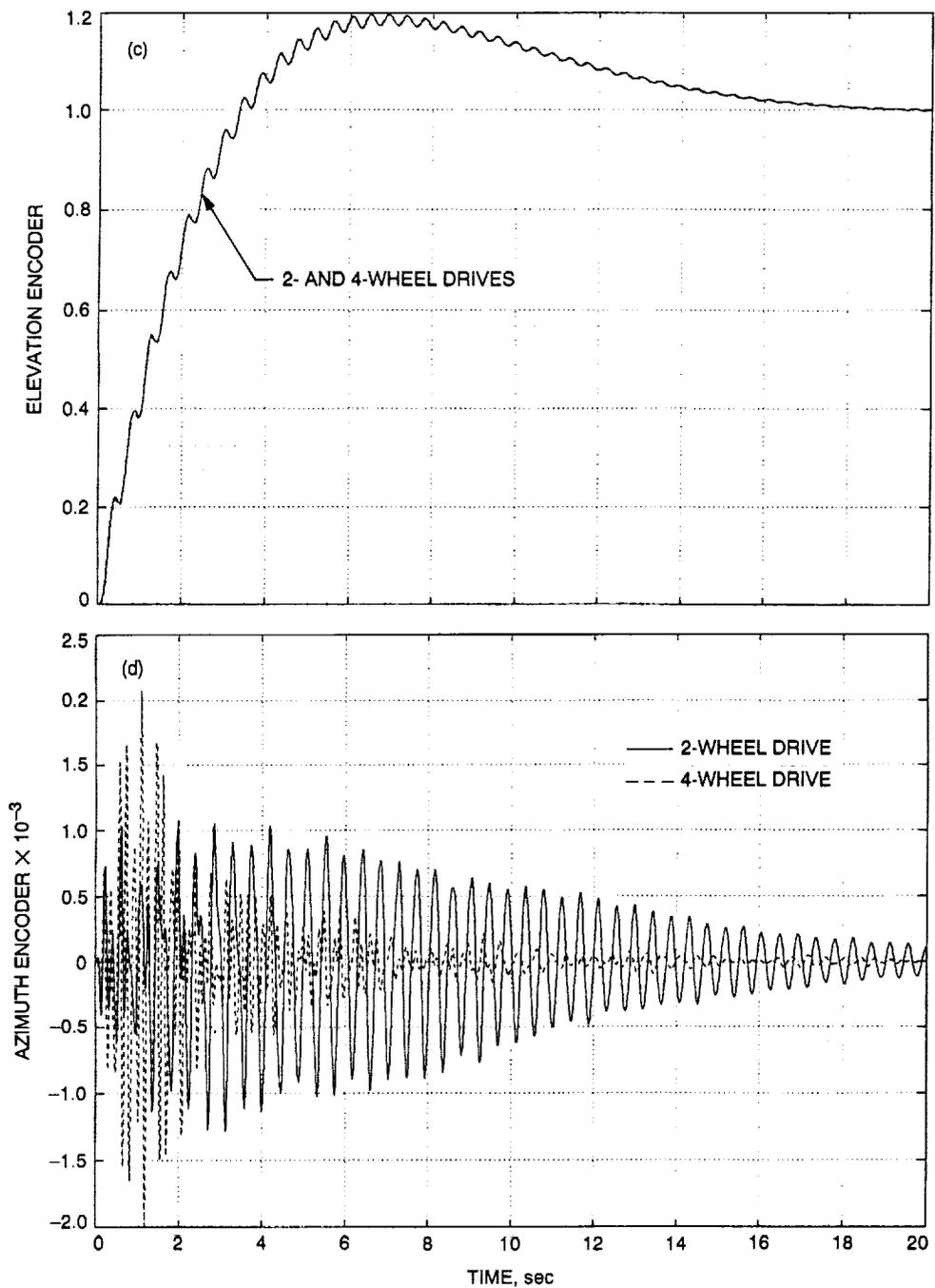
Fig. 9 (contd).
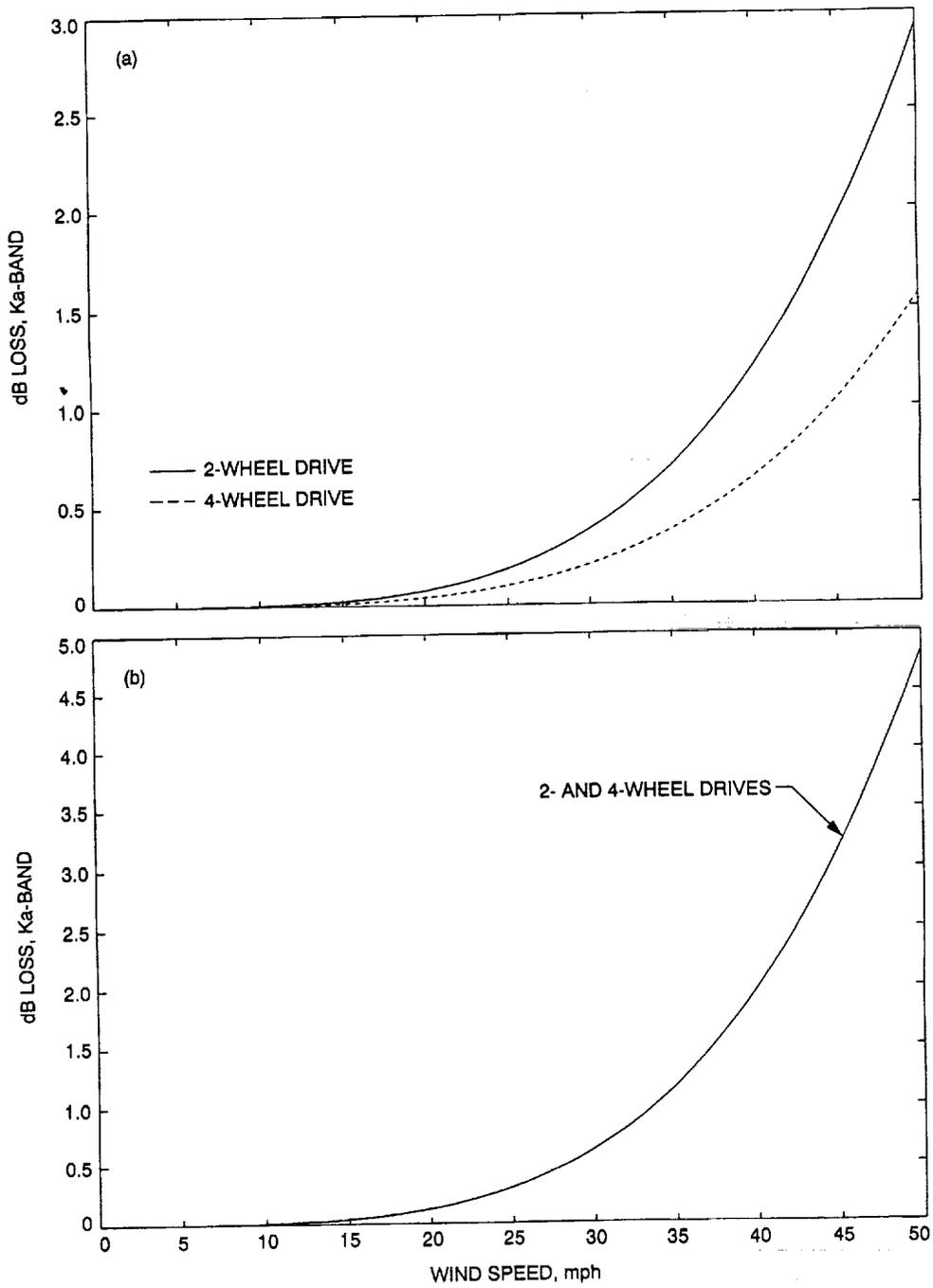
Fig. 10. Ka-band decibel loss due to wind gusts: (a) *x*-direction wind and (b) *y*-direction wind.